Hindawi
Complexity
Volume 2022, Article ID 7157524, 12 pages
https://doi.org/10.1155/2022/7157524

Research Article

Application of Flower Pollination Algorithm for Solving Complex Large-Scale Power System Restoration Problem Using PDFF Controllers

G. Ganesan Subramanian,[1] **Albert Alexander Stonier**,[2] **Geno Peter**,[3] **and Vivekananda Ganji**[4]

[1]*Department of Electrical and Electronics Engineering, E.G.S. Pillay Engineering College, Nagapattinam, Tamil Nadu, India*
[2]*Department of Electrical and Electronics Engineering, Kongu Engineering College, Perundurai, Tamil Nadu, India*
[3]*CRISD, School of Engineering and Technology, University of Technology Sarawak, Sarawak, Malaysia*
[4]*Department of Electrical and Computer Engineering, Debre Tabor University, Debre Tabor, Ethiopia*

Correspondence should be addressed to Vivekananda Ganji; drvivek@bhu.edu.et

Received 1 February 2022; Accepted 15 July 2022; Published 31 August 2022

Academic Editor: Qingling Wang

Automatic Generation Control (AGC) in modern power systems is getting complex, due to intermittency in the output power of multiple sources along with considerable digressions in the loads and system parameters. To address this problem, this paper proposes an approach to calculate Power System Restoration Indices (PSRI) of a 2-area thermal-hydro restructured power system. This study also highlights the necessary ancillary service requirements for the system under a deregulated environment to cater to large-scale power failures and entire system outages. An abrupt change in consumer load demands and disturbances in any control region (area) of a multiarea (interrelated) system causes severe fluctuations in frequency and interarea power exchanges. However, simple Proportional and Integral (PI) controllers are most prevalent in the literature to effectively resolve AGC issues, while its integral gain is smaller due to the larger overshoot in transient performance. Therefore, an attempt has been made with a novel control strategy, known as the pseudoderivative feedforward with feedback (PDFF) controller, is developed to keep the interarea power exchanges and the frequency to the specified limits after load changes. A PDFF controller is designed and implemented using the flower pollination algorithm (FPA) to obtain optimal dynamic performance for different types of potential power flows in a restructured power system under investigation. The proposed PDFF controller localizes the zero at an optimal place that reduces the rise time of the step-response to reduce the excessive overshoot and gives much better dynamic performances as compared to the PI control structure. The Integral Square Error (ISE) is considered as a performance criterion to derive the optimized gain of the PDFF control structure using FPA. Different PSRI are computed based on the transient response of the 2-area deregulated multisource system and different restoration measures to be taken are also discussed. The simulation results clearly show that the proposed approach is very powerful in decreasing the frequency and tie-power digressions under different load perturbations.

1. Introduction

Distribution, transmission, and generation of reliable electrical power are vital issues in energy management systems. The large-scale interrelated electric power systems can be divided into control regions that are interlinked using tie-lines [1]. These tie-lines are used to achieve power flow between the control regions and also to provide inter-region support in abnormal conditions. In an inter-related power system, as the load fluctuates arbitrarily at any one of the areas in the system, the system frequency, and tie-line power digresses from its standard value, which may cause detrimental impacts on a deregulated system. The AGC also named as load frequency control (LFC) is employed in such

conditions to reduce or eliminate the transitory abnormalities to keep the system frequency and voltage at nominal values and the power flow among various regions at their reserved values. Thus, an AGC is a significant control problem in the operation of the interconnected power system for delivering adequate and consistent power.

The joint effect of the deviations in system frequency and the interarea tie-line power exchanges is usually called as an area control error (ACE) [2, 3]. The objective of the controller is to reduce deviations in frequency from its standard value and to maintain interarea power transactions within the reserved values by minimizing the ACE. The value of ACE is then used by the subsequent sections of the control system, which will direct the governors of the different contributing generators to take necessary actions for decreasing or increasing generation.

The increasing complexities in the modern power system compelled researchers to develop appropriate control strategies for isolated as well as inter-related AGC in energy management systems. In state-of-the-art literature, several control schemes including integral (I), proportional-integral (PI), integral-derivative (ID), and proportional-integral-derivative (PID) have been developed to realize better system performance [4]. An integral part of ACE is considered as the control signal in traditional approaches for solving the AGC issue. Even though an integral controller can make the digressions in frequency and tie flow to settle to zero in the steady-state, it shows deprived transient response. The PI controllers are very effective in realizing frequency deviations settle to zero in the steady-state; however, it shows comparatively reduced transient response due to transient frequency fluctuations and large overshoot. Furthermore, PI controllers exhibit a degraded dynamic performance in terms of large oscillations and more settling time.

Under the new optimal control paradigm, the design of the control structure relies on a static parameter model using a linearization method. Generally, design constraints depend on the operating conditions. Hence, as the operating points vary, system enactment with control structures proposed for a particular condition probably will not be suitable. Therefore, the nonlinear characteristic of the AGC issue makes it challenging to guarantee steadiness for all conditions when an integral or a PI control structure is employed.

The derivative part of the PID controller increases the system reliability and improves the performance of the controller; however, it makes the generating unit consume a large control input. Besides, the noise signal leads to significant distortions, which frequently causes hitches in real-life implementation. The viable solution to this issue is to place a filter on the derivative section and optimize its gain values to eliminate high-frequency noise [5]. Hence, a PID with a derivative Filter (PIDF) controller is a good choice to solve the AGC problem under a restructured environment.

The application of flower pollination algorithm (FPA) for the power system studies is reviewed in [6]. The authors of this paper have already dealt with FPA-based PDFF algorithm for gas-diesel units in [7] where the computation has been made for Ancillary Service Requirement Assessment Indices (ASRAI) in lieu of Power System Restoration Indices (PSRI) for thermal-hydro system postulated in this paper. In addition, load frequency control (LFC) has been considered in [7] while Automatic Generation Control (AGC) is focused on in this paper.

The dynamic performance of automatic generation control (AGC) of two areas thermal–thermal power system is determined through the steam chest and re-heater constant trajectories in [8]. Here the controller gains are tuned using PSO (Particle Swarm Optimization) algorithm. A fuzzy-based controller for a two-area multisource thermal-hydro-gas and reheat thermal three-area systems are elucidated in [9].

In an extensive literature survey on AGC, mostly controllers like PID or PI with intelligent strategies are recommended [10–14], but the novelty of the proposed topology includes the PDFF control and gain optimization through FPA for a two-area thermal-hydro restructured power system.

In this paper, a Pseudoderivative Feedback with Feedforward (PDFF) control structure is proposed to enable more robust performance than that of the conventional controllers. The proposed PDFF adds the forward gain, which enables the client to increase the integral gain and delivers much better performance. The control parameters of the proposed control structure are optimized using FPA so as to realize the optimum transient response of the system for various types of possible transactions in a 2-area interrelated electrical power system.

2. Transfer Function Model of Power System in Deregulated Environment

An inter-related thermal-hydroelectric power system consisting of two generating units in each control region is considered. This system has two power plants in each region. Two reheat thermal power plants are considered in area-1 and area-2 contains one hydropower plant and a reheat thermal power plant. The comprehensive transfer function of steam and hydraulic turbines and their associated speed-governing systems are derived from the standards given by the IEEE Committee report [8]. Figure 1 depicts the transfer function model of the power system under investigation. It includes the transfer functions of thermal and hydro power plants along with the PDFF controllers.

3. Optimization of Design Parameters of PI and PDFF Controllers Using FPA

3.1. Control Structure of the PI Controller. Several controllers have been used in the design of AGC to obtain improved transient responses. The effective implementation of controllers will adjust the transient response and the error in a steady state. Amid the different types of structures, the conventional PI controller is widely used in AGC. In this paper, the best gains are optimized using the ACE signal (due to frequency and power digress from their standard values). In the feedback control structure, the controller is used to adapt the ACE and to realize improved control action. A feedback control strategy is used to activate the

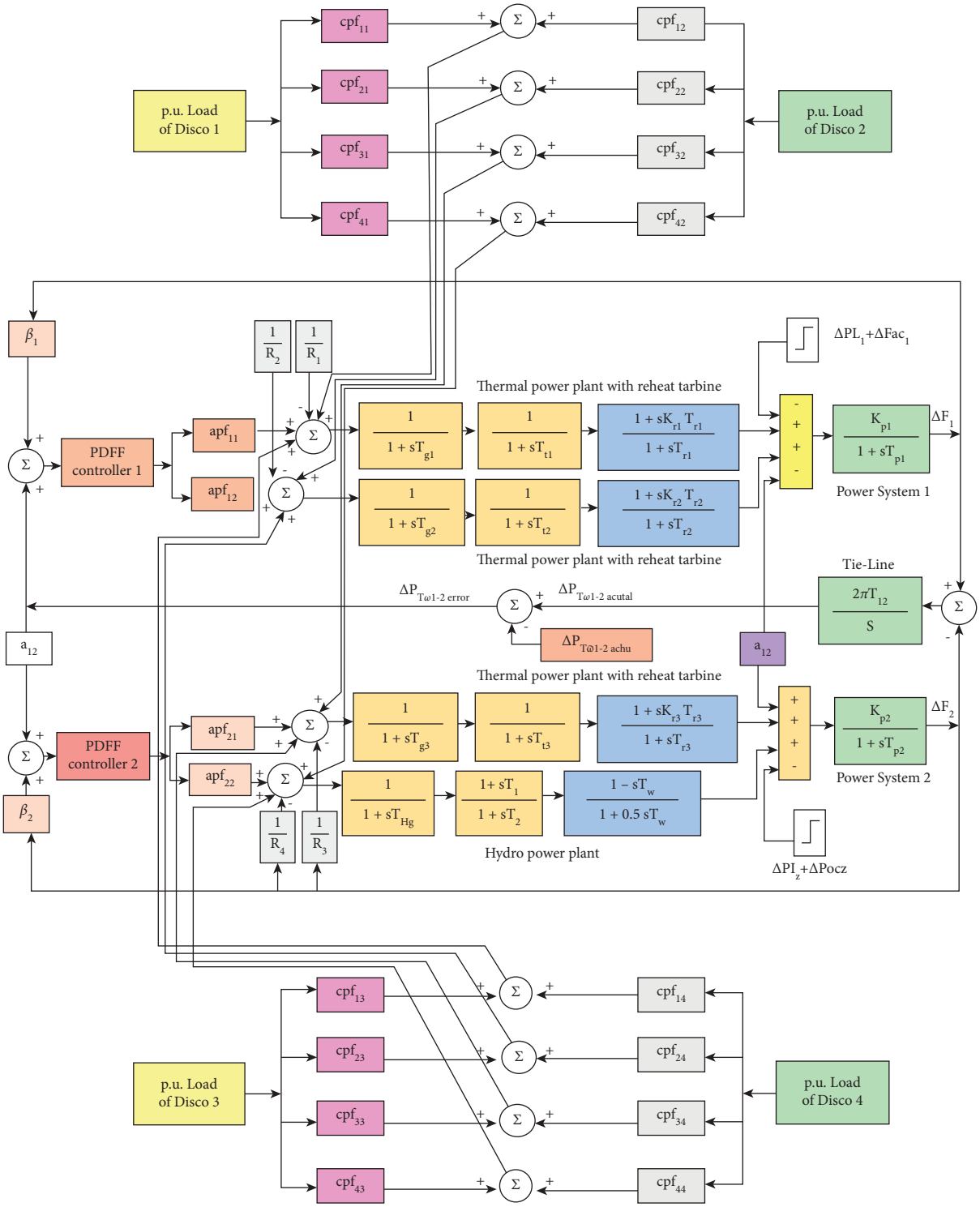

Figure 1: Transfer function model of the power system in a deregulated environment.

power system within a specified limit of error. The output of the PDFF controller consists of two terms. One term is associated with the error signal and another one is corresponding to its integral. To satisfy the above constraints, the proportional gain (K_{Pi}) and Integral gain (K_{Ii}) are to be optimized by means of FPA and uses an ISE measure to minimize the objective function.

The PI controller used for enhancing the transient response of AGC is given in Figure 2. The primary function of AGC is to reduce the dynamic digression in frequency and tie flow. Therefore, the error signals of these parameters are utilized as a design constraint for tuning the controller. ACE signals of the corresponding control area are generated by applying the error signal as defined in (1) and (2):

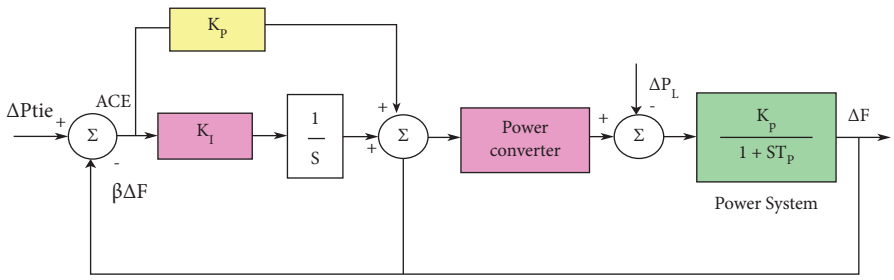

Figure 2: Configuration of the PI control structure.

$$ACE_1 = \beta_1 \Delta F_1 + \Delta P_{\text{Tie12}}^{\text{Error}}. \quad (1)$$

$$ACE_2 = \beta_2 \Delta F_2 + \alpha_{12} \Delta P_{\text{Tie12}}^{\text{Error}}. \quad (2)$$

The control inputs (i.e., u_1 and u_2) to the PI controller are shown in 3 and 4:

$$u_1 = K_{p1} ACE_1 + K_{I1} \int ACE_1 \mathrm{d}t. \quad (3)$$

$$u_2 = K_{p2} ACE_2 + K_{I2} \int ACE_2 \mathrm{d}t. \quad (4)$$

In this paper, FPA is employed to tune the gains of the proposed control structure. In order to optimize the gains of the PI controller, the minimization of ISE is considered as an objective function. The value of ISE is computed using the following equation:

$$J = \int_0^{t_{sim}} \left[(\beta \Delta F_1)^2 + (\beta \Delta F_2)^2 + (\Delta P_{tie})^2 \right] \mathrm{d}t. \quad (5)$$

The PI controller provides zero steady-state deviation. The dynamic enactment of the system is evaluated and different PSRI are computed using these optimized gain values.

3.2. Control Structure of the PDFF Controller. The proportional gain of a PI controller helps to achieve a high-frequency response, stability, and zero steady-state error. Therefore, there is no error when these gains are optimized properly. Hence, the responsiveness of the system is increased considerably. Conversely, the proportional-integral controller creates excessive overshoot frequently. Moreover, it cannot regulate the integral gain if the system is overloaded. Here, a PDFF controller is implemented to enable the user to remove or reduce overshoot. It delivers better DC stiffness than a conventional PI controller.

Figure 3 depicts the configuration of the PDFF control structure with the AGC loop. Similar to the PI controller, PDFF also has an integral gain (K_I) and proportional gain (K_P). This control structure also provides an additional gain KFR to enable the customer to increase the value of K_I in some solicitations. When an application needs higher responsiveness, then the K_I does not need much higher value. Here, KFR is set to a high value. When the application needs low-frequency stiffness, the KFR is set to a lower value; this enables maximum integral gain without leading to any overshoot. Regrettably, it slows down the system considerably. In most speed control applications, KFR is fixed at 65% to provide improved results. In this paper, the value of KFR is fixed to 0.65 then K_P and K_I values are optimized using FPA. The performance of the system is evaluated using equation (5).

4. Application of FPA for Scheming PI and PDFF Controllers

Optimization is the process of determining the optimal value of a set of variables to realize the goal of maximizing (or minimizing) an objective function subject to a specified set of restraints. Optimization is inherent in every walk of life ranging from our everyday life to commercial and business planning, and from industrial automation to engineering design. The input consists of variables; the function or process is called the cost (fitness/objective) function; the output is the cost or fitness function. Metaheuristics optimization is a sophisticated method that generates a simple procedure to handle an optimization problem [9–12]. It is described as a nondeterministic iterative method that acts as a controlling mechanism for the original heuristics by integrating several notions for exploiting and exploring the search space. In order to organize data for selecting near-optimal solutions effectively, learning approaches are implemented.

Metaheuristic algorithms are not problem-specific [1]. By searching over a large set of possible solutions, metaheuristics can determine better solutions with a reduced amount of computational complexity than algorithms, iterative generation processes, or rudimentary heuristics [13]. It is an enhancement to the comprehensive search that includes first searching a coarse sampling of the fitness function, then gradually narrowing the search to promising areas with a finer-toothed comb. It has better convergence characteristics. Furthermore, it increases the number of variables that can be examined but also increases the probabilities of missing the global minimum. Several metaheuristic approaches are inspired by some interesting characteristics of biological systems and are very effective in computing optimal solutions to complex problems. There are many such settings where the organisms (a swarm or a population) have optimized and improved themselves to stay alive in this biosphere (e.g., cuckoo algorithms, ant colony optimization, genetic algorithm,

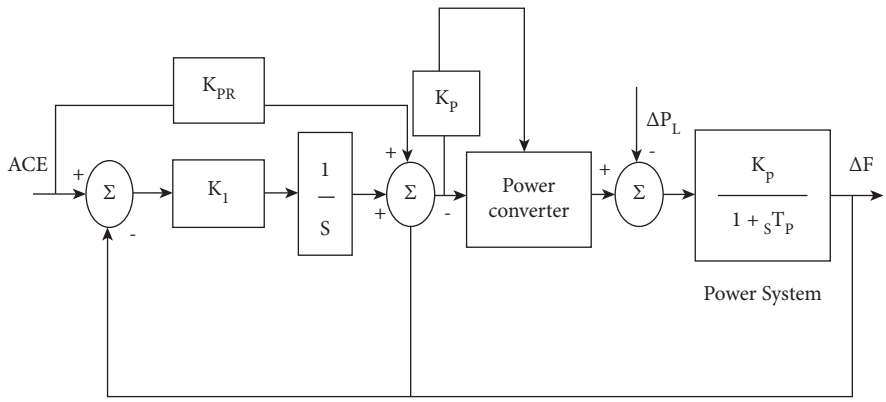

Figure 3: Configuration of the PDFF control structure.

and particle swarm optimization). The FPA is a new and versatile bio-inspired optimization method derived from the pollination behavior of flowering plants [14]. The reasons behind the success of FPA are flower stability and long-distance pollens [15, 16]. As stated by this algorithm, insects can travel distances, giving them the chance to escape any local landscape and giving them the aptitude to find out search space. This denotes the local search (exploration phase). Conversely, the stability of the flower represents selecting a particular type of flowers (i.e., similar solutions) regularly, and thus it rapidly ensures the added convergence, and this represents the global search (exploitation phase) [17]. The interaction between these key elements and the choice of the optimum solution proves that the algorithm is very effective [18–23].

The following steps describe the entire concept of FPA for solving the AGC problem:

(i) Define the objective function.

(ii) The FPA starts with random initialization of the population of $x = (x_1, x_2, \ldots, x_{NF})$. The size of the population is calculated from $NF \times N$. Here NF represents the total number of flowers considered (in this work $NF = 30$) and N denotes the number of gains of controllers for each control region. In the proposed work, N is equal to four because one PI controller is used in each area (K_{P1}, K_{I1}, K_{P2}, and K_{I2}) and evaluates the fitness of each solution.

(iii) Calculate the optimum value by considering the initial population and describe a change probability (i.e., $p \in [0, 1]$) and terminating condition.

(iv) While ($t <$ Maximum Generation) for $i = 1$ to n (i.e., n denotes number of flowers), if $p <$ rand, compute ε from a uniform distribution in [0, 1]. Else compute a d-dimensional vector L to perform global pollination. Select jth and kth flowers arbitrarily and perform local pollination, end if.

(v) Appraise solutions through the objective function. If the newly generated solutions are superior, apprise them in the population.

(vi) Determine the present optimum solution g according to the objective fitness cost, end while.

The flowchart of FPA-based optimization of the proposed controller for the AGC loop is shown in Figure 4.

5. Evaluation of PSRI

This work considers a 2-area interrelated system in a deregulated atmosphere. The PSRI of the system is computed as follows.

Stage 1: The PSRI_1 is calculated as the fraction of the settling time of input deviations and the power system time constant in control area-1.

$$\mathrm{PSRI}_1 = \frac{\Delta P_{c1}(\tau_{s1})}{TP_1}. \tag{6}$$

Stage 2: The PSRI_2 is defined as the fraction of the settling time of deviations in input deviations and the power system time constant in control area-2.

$$\mathrm{PSRI}_2 = \frac{\Delta P_{c2}(\tau_{s2})}{TP_2}. \tag{7}$$

Stage 3: The PSRI_3 is calculated from the deviations in the peak value of the input regarding its final value in control area-1.

$$\mathrm{PSRI}_3 = \Delta P_{c1}(\tau_p) - \Delta P_{c1}(\tau_s). \tag{8}$$

Stage 4: The PSRI4 is calculated from the deviation of the peak value of the input regarding its final value in control area-2.

$$\mathrm{PSRI}_4 = \Delta P_{c2}(\tau_p) - \Delta P_{c2}(\tau_s). \tag{9}$$

6. Simulation Results

In this paper, an interconnected thermal-hydroelectric power system is considered. This system has two power plants in each region. Two reheat thermal power plants are considered in area-1 and area-2 contains one hydropower plant and a

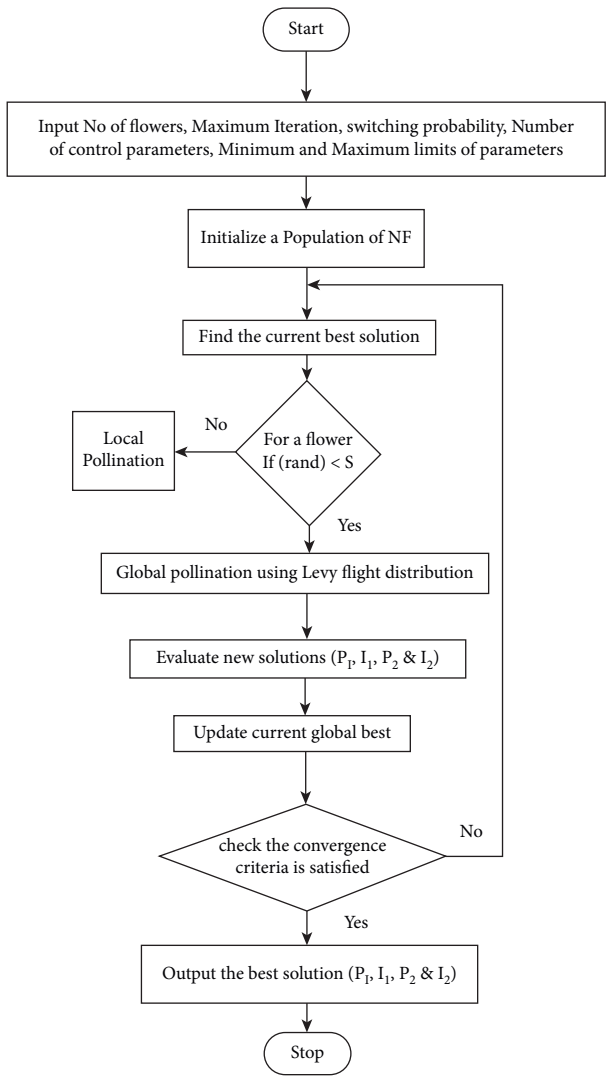

FIGURE 4: (a) Digression in the frequency of area-1 (Hz) vs time (s). (b) Digression in the frequency of area-2 (Hz) vs time (s). (c) Digression in tie-line power (p.u.MW) vs time (s). (d) Digression in control input (p.u.MW) in area-1 vs time (s). (e) Digression in control input (p.u.MW) in area-2 Vs time (s).

reheat thermal power plant. The nominal design constraints of the power system are given in the Appendix. The suggested control structures are developed and applied in an anticipated system for various exchanges. The design parameters of PI/PDFF are optimized by FPA. The selection of optimum input values is considered as a key issue and the objective function as given in (5) is derived to minimize oscillations in frequency and tie exchanges of control regions.

The optimum design parameters of control structures are computed for different contextual investigations and recorded in Tables 1 and 2. The controllers PI and PDFF are implemented in a power system to achieve various sorts of exchanges as shown in Table 3. From the simulation results, PSRI is computed using equations 6–9. The transient performance of the control input of the given system is shown in Table 4 (settings 1–4).

6.1. Scenario 1: Contracts Based on Poolco. In poolco-based exchanges, GenCos monitors the fluctuations in user demand in their control regions. Let us assume that there is a bulk load of 0.1 pu MW is required for each DisCo in area-1 and the contract between GenCos and Dicos is modeled using DisCo Participation Matrix (DPM) as given in the following equation:

$$\text{DPM} = \begin{bmatrix} 0.5 & 0.5 & 0.0 & 0.0 \\ 0.5 & 0.5 & 0.0 & 0.0 \\ 0.0 & 0.0 & 0.0 & 0.0 \\ 0.0 & 0.0 & 0.0 & 0.0 \end{bmatrix}. \tag{10}$$

DisCos (i.e., DisCo_1 and DisCo_2) request equal power from GenCos located within the control region. Hence, $cpf_{11} = cpf_{12} = cpf_{21} = cpf_{22} = 0.5$. It shows that none of the GenCos is agreed to supply this additional power and a DisCo breaks up an agreement by requesting extra power than the contracted power. The Genco located in the same region is responsible to deliver this power to the DisCo. This requested power is denoted as a claim of the control region but not as the agreement load.

6.2. Scenario 2: Bilateral Contracts. In this scenario, every DisCos has an agreement with the GenCos and the corresponding DPM is given in the following equation:

$$\text{DPM} = \begin{bmatrix} 0.4 & 0.2 & 0.4 & 0.5 \\ 0.1 & 0.3 & 0.2 & 0.3 \\ 0.3 & 0.2 & 0.2 & 0.1 \\ 0.2 & 0.3 & 0.2 & 0.2 \end{bmatrix}. \tag{11}$$

In this scenario, the DisCo_1 and DisCo_3 demand 0.15 pu.MW and DisCo_2 and DisCo_4 demand 0.05 pu MW from GenCos as indicated in the DPM and each GenCos contributes in generation control activities as described by ACE participation factors $apf_{11} = apf_{12} = apf_{21} = apf_{22} = 0.5$. From the simulation, the results of PSRI are assessed using equations (6)–(9). The transient performance of the control input of the proposed test system is shown in Table 4 (settings 5–8).

Several investigations have been carried out on operating condition-based restoration strategies. Some setting studies involve blackouts in power plants and uncontracted power requests from any region during a blackout. In order to construct DPM in the present work, it is assumed that Genco-4 in area-2 is a blackout and the system can receive uncontracted power requests from any region. The optimum gain values of PI and PDFF controllers are presented in Tables 1 and 2 correspondingly (settings 9–12). The proposed control structures are applied for a variety of transactions and the dynamic performance is given in Figure 5. The PSRI is computed and presented in Table 4. It is evident from the results that the restoration method with the PDFF controller guarantees not only steady-state function but also delivers a better stability margin related to that of a PI controller.

Table 1: Optimized PI controller gains for the power system under investigation.

2-area system	Gain of PI controller in area-1		Gain of PI controller in area-2		Demand in pu.MW				Uncontracted demand pu.MW	
	K_P	K_I	K_P	K_I	$DisCo_1$	$DisCo_2$	$DisCo_3$	$DisCo_4$	Area-1	Area-2
Setting 1	0.314	0.419	0.263	0.354	0.10	0.10	0.00	0.00	0.00	0.00
Setting 2	0.333	0.448	0.278	0.367	0.10	0.10	0.00	0.00	0.04	0.00
Setting 3	0.364	0.437	0.294	0.344	0.10	0.10	0.00	0.00	0.00	0.04
Setting 4	0.385	0.493	0.298	0.373	0.10	0.10	0.00	0.00	0.04	0.04
Setting 5	0.319	0.364	0.284	0.375	0.14	0.04	0.14	0.04	0.00	0.00
Setting 6	0.334	0.373	0.392	0.376	0.14	0.04	0.14	0.04	0.04	0.00
Setting 7	0.348	0.363	0.393	0.384	0.14	0.04	0.14	0.04	0.00	0.04
Setting 8	0.412	0.383	0.417	0.394	0.14	0.04	0.14	0.04	0.04	0.04
Setting 9	0.345	0.364	0.427	0.393	0.11	0.07	0.11	0.07	0.00	0.00
Setting 10	0.367	0.378	0.431	0.444	0.11	0.07	0.11	0.07	0.04	0.00
Setting 11	0.369	0.418	0.438	0.481	0.11	0.07	0.11	0.07	0.00	0.04
Setting 12	0.388	0.443	0.447	0.490	0.11	0.07	0.11	0.07	0.04	0.04

Table 2: Optimized PDFF controller gains for the power system under investigation.

2-area system	PDFF controller gains of area-1 with KFR = 0.65.		PDFF controller gain of area-2 with KFR = 0.65.		Demand in pu.MW				Demand uncontracted pu.MW	
	K_P	K_I	K_P	K_I	DisCo1	DisCo2	DisCo3	DisCo4	Area-1	Area-2
Setting 1	0.289	0.408	0.248	0.345	0.10	0.10	0.00	0.00	0.00	0.00
Setting 2	0.310	0.429	0.263	0.351	0.10	0.10	0.00	0.00	0.06	0.00
Setting 3	0.339	0.425	0.279	0.329	0.10	0.10	0.00	0.00	0.00	0.06
Setting 4	0.359	0.490	0.282	0.357	0.10	0.10	0.00	0.00	0.06	0.06
Setting 5	0.307	0.352	0.263	0.355	0.14	0.06	0.14	0.06	0.00	0.00
Setting 6	0.313	0.359	0.381	0.352	0.14	0.06	0.14	0.06	0.06	0.00
Setting 7	0.328	0.351	0.375	0.369	0.14	0.06	0.14	0.06	0.00	0.06
Setting 8	0.399	0.369	0.395	0.371	0.14	0.06	0.14	0.06	0.06	0.06
Setting 9	0.328	0.361	0.381	0.375	0.13	0.09	0.12	0.09	0.00	0.00
Setting 10	0.349	0.372	0.396	0.427	0.13	0.09	0.12	0.09	0.06	0.00
Setting 11	0.357	0.393	0.391	0.471	0.13	0.09	0.12	0.09	0.00	0.06
Setting 12	0.363	0.419	0.409	0.475	0.13	0.09	0.12	0.09	0.06	0.06

Table 3: Comparison of the system dynamic performance of the power system under investigation with different controllers (Setting 1).

Controller design	Setting time (τ_s) in sec			Peak over/undershoot		
	$\Delta F1$	$\Delta F2$	ΔP_{tie}	$\Delta F1$ in Hz	$\Delta F2$ in Hz	ΔP_{tie} in p.u.MW
PI controller	25.9	22.8	38.4	0.315	0.261	0.077
PDFF controller	20.5	18.6	35.7	0.239	0.147	0.054

Table 4: PSRI of the power system under investigation for a different type of controller.

Load demand change	PSRI of the system with PI controller					PSRI of the system with PDFF controller				
	$PSRI_1$	$PSRI_2$	$PSRI_3$	$PSRI_4$	$\int P_{c2}$	$PSRI_1$	$PSRI_2$	$PSRI_3$	$PSRI_4$	$\int P_{c2}$
Setting 1	1.606	1.601	0.098	0.033	0.322	1.595	1.508	0.095	0.031	0.264
Setting 2	1.927	1.722	0.134	0.053	0.417	1.845	1.623	0.108	0.032	0.345
Setting 3	1.863	1.872	0.107	0.042	3.523	1.784	1.678	0.096	0.036	3.467
Setting 4	2.318	2.171	0.137	0.046	3.937	2.237	2.073	0.127	0.043	3.872
Setting 5	1.557	1.674	0.106	0.038	1.902	1.478	1.578	0.091	0.032	1.784
Setting 6	1.626	1.887	0.113	0.043	1.761	1.547	1.789	0.109	0.037	1.687
Setting 7	1.836	1.973	0.118	0.046	3.604	1.758	1.875	0.104	0.039	3.523
Setting 8	1.924	2.072	0.124	0.044	3.311	1.845	1.978	0.112	0.041	3.124
Setting 9	2.132	2.377	1.168	0.059	1.619	2.051	2.278	1.142	0.057	1.437
Setting 10	2.208	2.475	1.175	0.062	1.785	2.127	2.378	1.157	0.058	1.594
Setting 11	2.426	2.556	1.181	0.067	3.875	2.347	2.458	1.158	0.059	3.696
Setting 12	3.055	2.971	1.269	0.071	3.861	2.972	2.879	1.245	0.061	3.688

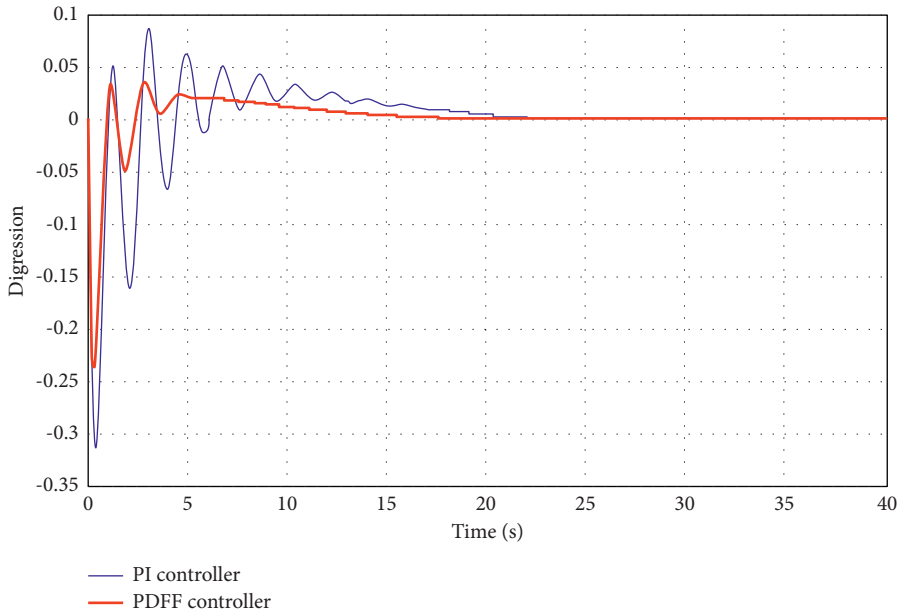

(a)

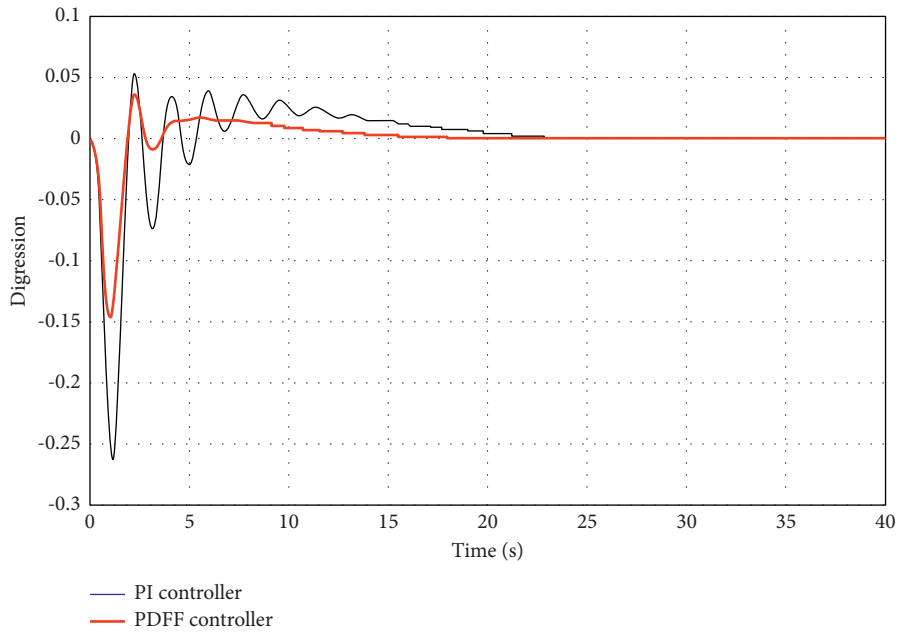

(b)

Figure 5: Continued.

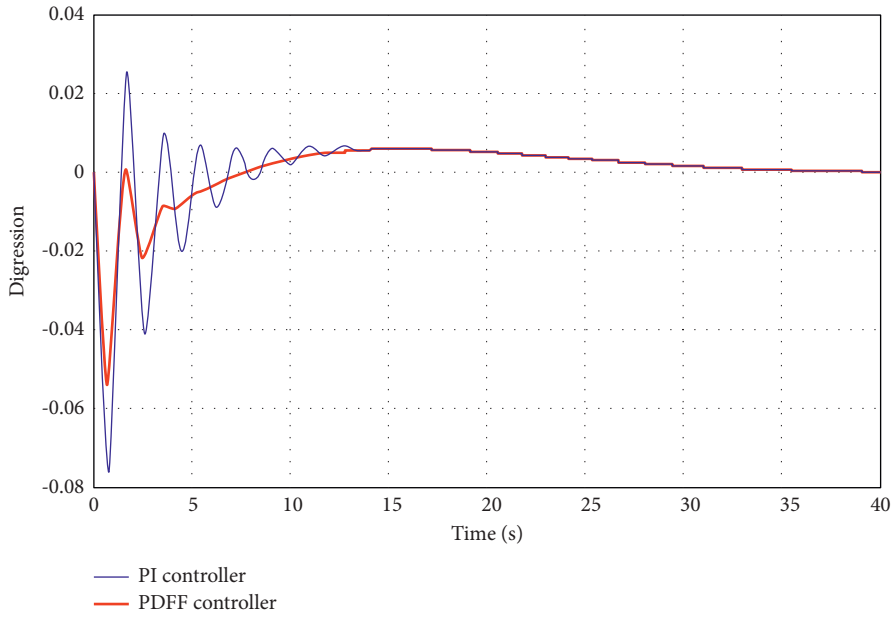

(c)

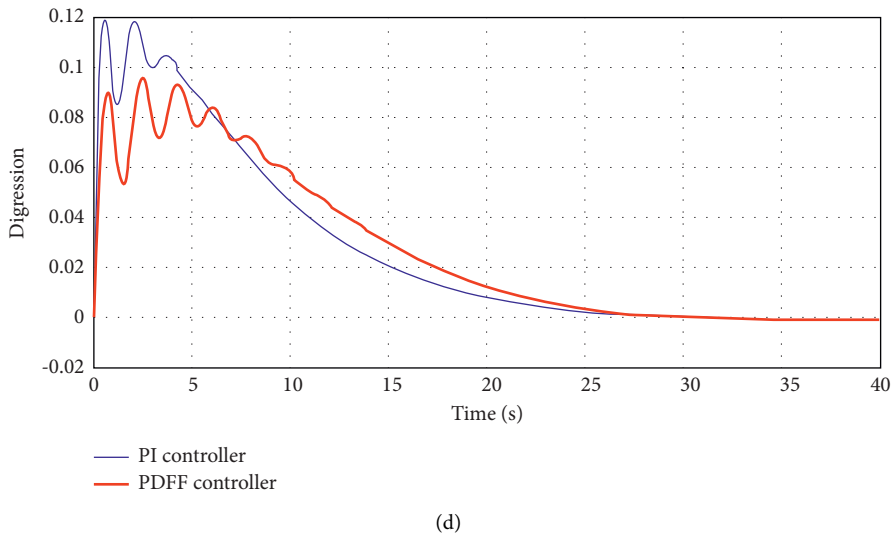

(d)

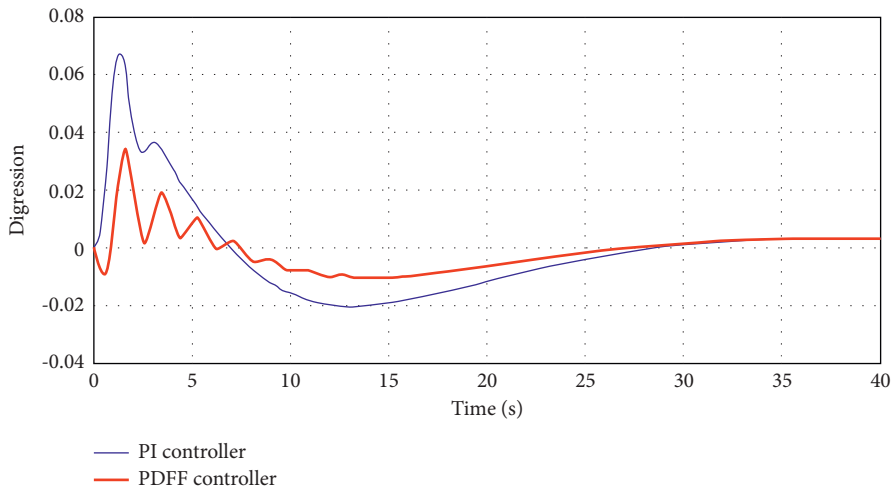

(e)

Figure 5: Flowchart for optimizing the parameters of PI controller using FPA.

Table 5: Comparative analysis with the existing systems.

Reference	Configuration	Controller	Peak overshoot			Settling time		
			$\Delta F1$	$\Delta F2$	ΔP_{tie}	$\Delta F1$ in Hz	$\Delta F2$ in Hz	ΔP_{tie} in p.u.MW
[19]	Two areas nonreheat thermal power system	DE-based 2DOF-PID regulator	0.0144	0.00598	0.00711	11.1	7.2	13.8
[20]	Two area nonreheat thermal power system	ACO-based PID regulator	1.1×10^{-6}	0.0002	0.0001	29.62	37.20	50.41
[26]	Two areas reheat thermal, hydro, gas, and nuclear power plant	TLBO-based AGC system with output feedback SMC	0.0016	4.301×10^{-4}	8.050×10^{-5}	1.52	1.54	1,24
[22]	Two areas reheat thermal, hydro, gas, and nuclear power plant	LUS-TLBO-based fuzzy PID controller	0.000551	0.000219	0.0000826	5.26	2.96	2.36
Proposed	Two areas thermal-hydro	PDFF with FPA	20.5	18.6	35.7	**0.239**	**0.147**	**0.054**

The significance of the bold values given in Table 5 is that in the proposed method, settling time is much less when compared to other conventional systems.

The basis for simulations setting is as follows: The variation of frequency in Hz with respect to time for the two different controllers such as PI and the proposed PDFF is analyzed for the area-1 and area-2 as illustrated in Figure 4. The variation in a different setting is achieved by changing the controller gains of the respective controllers.

7. Evaluation of Restoration in Deregulated Atmosphere

PSRI of an inter-related electrical system can be used for (i) automatic power system restructuring, (ii) enabling operators to take necessary actions immediately, and (iii) off-line scheduling for restructuring before the expected shutdown. This considers various restructuring approaches/schemes and relates restoration phases after alterations. The objective of this article is to ensure restoration planning earlier.

(i) When $1.0 \leq [\ (\text{PSRI})\ ]\_1$, and $[\ (\text{PSRI})\ ]\_2 \leq 2.0$, the power system experiences a huge steady-state error for input variations. A counter-reactive action is essential according to the operating condition. The gain of the integral controller must be improved for triggering the speed limiter valve to open up. In this manner, the position of the speed-changer accomplishes a fixed value when the deviation in frequency is decreased to zero.

(ii) When $[\ (\text{PSRI})\ ]\_1$, $[\ (\text{PSRI})\ ]\_2 \geq 2.0$, the power system needs a greater number of distributed generation and the Flexible Alternating Current Transmission Systems (FACTS) controller are anticipated to eliminate tie-line power fluctuations.

(iii) When $0.05 \leq [\ (\text{PSRI})\ ]\_3$, $[\ (\text{PSRI})\ ]\ \_4 \leq 0.1$, the interconnected power system need the frequency stabilization for its successful operation. The traditional AGC with a slow response governor cannot reduce the frequency digression for arbitrary demand fluctuations. Modern high-speed energy storage technology consists of a storage facility for dynamic energy of the plant is desirable to ensure frequency stability. In an interconnected system, load following and regulation are important ancillary facilities that are mandatory for compensating the fluctuating user demand with synchronizing generation. The activities on the interrelated power system to enable the active power transmission while preserving stable operation, necessary quality level, and safety is known as ancillary services.

(iv) When $[\ (\text{PSRI})\ ]\_3$, $[\ (\text{PSRI})\ ]\_4 \leq 0.2$, the power system is susceptible and it becomes unstable and may lead to shut down. To cope with restoration scenarios as quickly as possible the operators ought to set restoration policies and recommendations for some usual blackout conditions. The operators have to implement these strategies in the present scenario with the consideration of two key approaches in restoration which can be defined as top-down and bottom-up. In the bottom-up approach, a number of minor electrical islands or subsystems are operated concurrently. Then, these subsystems are employed to drive the transmission system. At the same time, the synchronization of the subsystems decelerates the system's operation. In the top-down approach, the transmission system is driven from a particular place and the remaining units are operated by the transmission system. Then, the entire deregulated energy system is coordinated.

With reference to the analysis made and based on the results obtained, it is found that the computation of different PSRI based on the transient response of the 2-area deregulated multisource system results in the multiple restoration measures to be undertaken. The simulation results clearly show that the proposed approach is very powerful in decreasing the frequency and tie-power digressions under different load perturbations. The performance of PDFF makes much superior to that of PI in terms of analysis, settling time, and relative performance. Table 5 shows the comparative analysis of the proposed methodology with the conventional systems.

8. Conclusion

This paper discussed the simulation studies that have been performed on a 2-area thermal-hydro deregulated power system to explore the effect of the proposed control structure, PDFF controller, on the improvement of power system transient responses. The PDFF controller with a low pass filter is intended to eliminate or reduce the overshoot in the AGC problem. The gains of a PDFF control structure are optimized using FPA in order to obtain optimal dynamic performance for different types of potential power flows in a restructured power system under investigation. The proposed PDFF controller localizes the zero at an optimal place that reduces the rise time of the step-response in order to reduce the excessive overshoot and gives much better dynamic performances as compared to the PI controller. The ISE is considered as a performance criterion to derive the optimized gain of the PDFF control structure using FPA. Different PSRI is computed based on the transient response of the 2-area deregulated multisource system and discuss different restoration measures to be taken. The simulation results clearly show that the proposed approach is very powerful in decreasing the frequency and tie-power digressions under different load perturbations.

Appendix

(i) Area-1: Thermal Power Plant [23].

Rating of each area = 2000 MW
Base power = 2000 MVA
$f_o = 60$ Hz
$R_1 = R_2 = 5$ Hz/pu.MW
$T_{g1} = T_{g2} = 0.25$ s
$T_{r1} = T_{r2} = 10$ s
$T_{t1} = T_{t2} = 0.25$ s
$K_{p1} = K_{p2} = 120$ Hz/pu.MW
$T_{p1} = T_{p2} = 20$ s
$\beta_1 = \beta_2 = 0.2083$ pu.MW/Hz
$K_{r1} = K_{r2} = 0.5$
$a_{12} = -1$
$\Delta P_{D1} = 0.01$ pu MW

(ii) Area-2: Hydropower Plant [23].

Rating of each area = 200 MW
Base power = 200 MVA
$f_0 = 60, T_{\mathrm{Hg}} = 0.2$ s
$T_1 = 0.513$ s
$T_2 = 10$ s
$T_w = 1$ s
$R_1 = 5$ Hz/*p*u.MW
$R_2 = 2.4$ Hz/*p*u.MW
$T_{g1} = 0.25$ s
$T_{r1} = 10$ s
$Tt_1 = 0.25$ s
$T_2 = 10$ s
$T_w = 1$ s
$R_1 = 5$ Hz/*p*u.MW
$R_2 = 2.4$ Hz/.u.MW
$T_{g1} = 0.25$s
$T_{r1} = 10$ s
$T_{t1} = 0.25$ s
$K_{p1} = K_{p2} = 120$ Hz/*p*u.MW
$T_{p1} = T_{p2} = 20$ s
$\Delta P_{D1} = 0.2083$ pu.MW/Hz
$K_{r1} = 0.5$

Data Availability

The required data can be obtained from the corresponding author upon request.

Conflicts of Interest

The authors declare that they have no conflicts of interest.

Acknowledgments

The writing and editing of this study was supported by Debre Tabor University, Ethiopia.

References

[1] I. A. Chidambaram and B. Paramasivam, "Optimized load-frequency simulation in restructured power system with redox flow batteries and interline power flow controller," *International Journal of Electrical Power & Energy Systems*, vol. 50, pp. 9–24, 2013.

[2] L. C. Saikia, J. Nanda, and S. Mishra, "Performance comparison of several classical controllers in AGC for multi-area interconnected thermal system," *International Journal of Electrical Power & Energy Systems*, vol. 33, no. 3, pp. 394–401, 2011.

[3] V. Donde, M. A. Pai, and I. A. Hiskens, "Simulation and optimization in an AGC system after deregulation," *IEEE Transactions on Power Systems*, vol. 16, no. 3, pp. 481–489, 2001.

[4] L. C. Saikia and S. K. Sahu, "Automatic generation control of a combined cycle gas turbine plant with classical controllers using firefly algorithm," *International Journal of Electrical Power & Energy Systems*, vol. 53, pp. 27–33, 2013.

[5] R. K. Sahu, S. Panda, and S. Padhan, "Optimal gravitational search algorithm for automatic generation control of interconnected power systems," *Ain Shams Engineering Journal*, vol. 5, no. 3, pp. 721–733, 2014.

[6] S. Lalljith, I. Fleming, U. Pillay, K. Naicker, Z. J. Naidoo, and A. K. Saha, "Applications of flower pollination algorithm in electrical power systems: a review," *IEEE Access*, vol. 10, pp. 8924–8947, 2022.

[7] G. G. Subramanian, I. A. Chidambaram, and J. S. Manoharan, "Flower pollination algorithm based PDFF controller for a two-area interconnected thermal power system with gas/diesel units," *Global Journal of Energy Technology Research Updates*, vol. 4, pp. 26–34, 2017.

[8] N. Pathak, T. S. Bhatti, A. Verma, and I. Nasiruddin, "AGC of two area power system based on different power output control strategies of thermal power generation," *IEEE Transactions on Power Systems*, vol. 33, no. 2, pp. 2040–2052, March 2018.

[9] P. Geno, "A review about vector group connections in transformers," *International Journal of Advancements in Technology*, vol. 2, no. No. 2, pp. 0976–4860, 2011.

[10] R. K. Sahu, S. Panda, and G. T. Chandra Sekhar, "A novel hybrid PSO-PS optimized fuzzy PI controller for AGC in multi area interconnected power systems," *International Journal of Electrical Power & Energy Systems*, vol. 64, pp. 880–893, 2015.

[11] Y. Arya, N. Kumar, P. Dahiya et al., "Cascade-I $^{\lambda}$ D $^{\mu}$ N controller design for AGC of thermal and hydro-thermal power systems integrated with renewable energy sources," *IET Renewable Power Generation*, vol. 15, no. 3, pp. 504–520, 2021.

[12] N. C. Patel, B. K. Sahu, D. P. Bagarty, P. Das, and M. K. Debnath, "A novel application of ALO-based fractional order fuzzy PID controller for AGC of power system with diverse sources of generation," *International Journal of Electrical Engineering Education*, vol. 58, no. 2, pp. 465–487, 2021.

[13] Y. Arya, "AGC performance enrichment of multi-source hydrothermal gas power systems using new optimized FOFPID controller and redox flow batteries," *Inside Energy*, vol. 127, pp. 704–715, 2017.

[14] G. Peter and S. Bin Iderus, "Design of enhanced energy meter using GSM prepaid system and protective relays," *Materials Today Proceedings*, vol. 39, pp. 582–589, 2021.

[15] I. C. Report, "Dynamic models for steam and hydro turbines in power system studies," *IEEE Transactions on Power Apparatus and Systems*, vol. PAS-92, no. 6, pp. 1904–1915, 1973.

[16] R. Roy, P. Bhatt, and S. P. Ghoshal, "Evolutionary computation based three-area automatic generation control," *Expert Systems with Applications*, vol. 37, no. 8, pp. 5913–5924, 2010.

[17] S. Manna, G. Mani, S. Ghildiyal et al., "Ant colony optimization tuned closed-loop optimal control intended for vehicle active suspension system," *IEEE Access*, vol. 10, pp. 53735–53745, 2022.

[18] M. Omar, M. Soliman, A. M. A. Ghany, and F. Bendary, "Optimal tuning of PID controllers for hydrothermal load frequency control using ant colony optimization," *International Journal on Electrical Engineering and Informatics*, vol. 5, no. 3, pp. 348–360, 2013.

[19] A. Rahman, L. C. Saikia, and N. Sinha, "Load frequency control of a hydro-thermal system under deregulated environment using biogeography based optimised three degree of freedom integral derivative controller," *IET Generation, Transmission & Distribution*, vol. 9, no. 15, pp. 2284–2293, 2015.

[20] G. Peter and A. Sherine, "Induced over voltage test on transformers using enhanced Z-source inverter based circuit," *Journal of Electrical Engineering*, vol. 68, no. 5, pp. 378–383, 2017.

[21] A. E. Kayabekir et al., "A comprehensive review of the flower pollination algorithm for solving engineering problems," in *Nature-Inspired Algorithms and Applied Optimization*, X. S. Yang, Ed., pp. 171–188, Springer, Cham, 2018.

[22] Z. A. A. Alyasseri, A. T. Khader, M. A. Al-Betar, M. A. Awadallah, and X.-S. Yang, "Variants of the flower pollination algorithm: a review," in *Nature-Inspired Algorithms and Applied Optimization*, X. S. Yang, Ed., , pp. 91–118, Springer, 2018.

[23] G. Peter, K. Praghash, A. Sherine, and V. Ganji, "A combined PWM and AEM-based AC voltage controller for resistive loads," *Mathematical Problems in Engineering*, vol. 2022, pp. 1–11, 2022.

[24] S. K. P. Mishra and S. Sekhar, "Modelling of differential evolution based automatic generation control for two area interconnected power systems," *J. Inform. Math. Sci.*vol. 11, pp. 19–30, 2019.

[25] K. Jagatheesan, B. Anand, K. N. Dey, A. S. Ashour, and S. C. Satapathy, "Performance evaluation of objective functions in automatic generation control of thermal power system using ant colony optimization technique-designed proportional–integral–derivative controller," *Electrical Engineering*, vol. 100, no. 2, pp. 895–911, 2018.

[26] B. Mohanty, "TLBO optimized sliding mode controller for multi-area multi-source nonlinear interconnected AGC system," *International Journal of Electrical Power & Energy Systems*, vol. 73, pp. 872–881, 2015.

[27] B. K. Sahu, T. K. Pati, J. R. Nayak, S. Panda, and S. K. Kar, "A novel hybrid LUS–TLBO optimized fuzzy-PID controller for load frequency control of multi-source power system," *International Journal of Electrical Power & Energy Systems*, vol. 74, pp. 58–69, 2016.

[28] A. Kumar, O. P. Malik, and G. S. Hope, "Variable-structure-system control applied to AGC of an interconnected power system," *IEE Proceedings C Generation, Transmission and Distribution*, vol. 132, no. 1, pp. 23–29, 1985.